JOURNAL OF BACTERIOLOGY, Oct. 1999, p. 6254–6263 Vol. 181, No. 20
0021-9193/99/$04.00+0

Cloning and Sequence Analysis of Two *Pseudomonas* Flavoprotein Xenobiotic Reductases

DAVID S. BLEHERT,[1] BRIAN G. FOX,[2]* AND GLENN H. CHAMBLISS[1]*

Department of Bacteriology, Graduate School and College of Agricultural and Life Sciences, University of Wisconsin, Madison, Wisconsin 53706,[1] and Institute for Enzyme Research and Department of Biochemistry, Graduate School and College of Agricultural and Life Sciences, University of Wisconsin, Madison, Wisconsin 53705[2]

Received 21 May 1999/Accepted 30 July 1999

The genes encoding flavin mononucleotide-containing oxidoreductases, designated xenobiotic reductases, from *Pseudomonas putida* II-B and *P. fluorescens* I-C that removed nitrite from nitroglycerin (NG) by cleavage of the nitroester bond were cloned, sequenced, and characterized. The *P. putida* gene, *xenA*, encodes a 39,702-Da monomeric, NAD(P)H-dependent flavoprotein that removes either the terminal or central nitro groups from NG and that reduces 2-cyclohexen-1-one but did not readily reduce 2,4,6-trinitrotoluene (TNT). The *P. fluorescens* gene, *xenB*, encodes a 37,441-Da monomeric, NAD(P)H-dependent flavoprotein that exhibits fivefold regioselectivity for removal of the central nitro group from NG and that transforms TNT but did not readily react with 2-cyclohexen-1-one. Heterologous expression of *xenA* and *xenB* was demonstrated in *Escherichia coli* DH5α. The transcription initiation sites of both *xenA* and *xenB* were identified by primer extension analysis. BLAST analyses conducted with the *P. putida xenA* and the *P. fluorescens xenB* sequences demonstrated that these genes are similar to several other bacterial genes that encode broad-specificity flavoprotein reductases. The prokaryotic flavoprotein reductases described herein likely shared a common ancestor with old yellow enzyme of yeast, a broad-specificity enzyme which may serve a detoxification role in antioxidant defense systems.

Xenobiotic compounds containing nitro functional groups are used in the production of explosives, agricultural chemicals, pharmaceuticals, dyes, and plastics (14, 37, 44). Through their industrial production and use, nitro-substituted compounds have been introduced into the environment over the last several decades. Recently, bacterial transformations of nitro-substituted compounds found in the soil and groundwater surrounding munitions manufacturing plants have been demonstrated (4, 5, 13, 26, 31, 43, 45). These studies have focused on two distinct classes of compounds, aliphatic nitroesters including nitroglycerin (NG; glycerol trinitrate) and pentaerythritol tetranitrate (PETN), and nitroaromatic compounds including 2,4,6-trinitrotoluene (TNT) and isomers of dinitrotoluene. The bacterial transformation of nitro-substituted xenobiotics highlights the remarkable capacity of bacteria to adapt metabolic pathways to degrade novel compounds.

The best-characterized biological transformation of a nitro-substituted compound is the reduction of the electrophilic nitro group of a nitroaromatic compound such as TNT. Spain has proposed that the majority of living organisms possess enzymes, referred to as nitroreductases, that catalyze this transformation (37). The most thoroughly characterized group of nitroreductases, the oxygen-insensitive type I nitroreductases, reduce nitroaromatic compounds through successive two-electron reductions of the nitro group (compound 1) to nitroso (compound 2), hydroxylamino (compound 3), and ultimately amino (compound 4) substituents (Fig. 1A). The type I nitroreductases are either monomeric or homodimeric flavin mononucleotide (FMN)-containing flavoproteins with a subunit size of approximately 25 kDa and use NAD(P)H as a reductant.

Recent studies of the biological transformation of aliphatic nitroester compounds such as NG and PETN have revealed another class of bacterial flavoproteins. These FMN-containing flavoproteins catalyze the NAD(P)H-dependent cleavage of nitro groups from NG, releasing nitrite (Fig. 1B). We recently reported the purification and characterization of the flavoprotein nitroester reductases from two different species of *Pseudomonas* isolated from munitions-contaminated soil (5). Other groups have characterized biochemically similar bacterial flavoproteins that react with NG, PETN (4, 36), and other electrophilic xenobiotics, including 2-cyclohexen-1-one (Fig. 1C), *N*-ethylmaleimide, morphinone and codeinone, and TNT (12, 13, 28, 32). A comparison of biochemical traits of these flavoproteins reveals that all except the homodimeric morphinone reductase are monomeric enzymes with a subunit size of approximately 40 kDa. Since the substrates identified for this enzyme family are primarily xenobiotics, herein we will refer to these enzymes as xenobiotic reductases.

The best-characterized protein sharing biochemical properties and sequence similarity with the bacterial xenobiotic reductases is old yellow enzyme (OYE), a dimeric, FMN-containing flavoprotein identified in several species of yeast (18). Although OYE has been extensively characterized (1, 18, 20, 25, 33, 35) and the crystal structure of OYE has been solved (11), the physiological role of OYE has remained obscure. OYE reacts with several substrates, catalyzing the reduction of quinones, as well as the reduction of the olefinic bond of α,β-unsaturated aldehydes and ketones (18). Most recently, Kohli and Massey hypothesized that these interactions with electrophilic substrates indicate that OYE may serve as a detoxification enzyme in antioxidant defense systems (20).

In this work, we describe the cloning and characterization of the *xenA* (xenobiotic reductase A) and *xenB* (xenobiotic reductase B) genes of *Pseudomonas putida* II-B and *P. fluorescens*

* Corresponding author. Mailing address for Brian G. Fox: Institute for Enzyme Research, 1710 University Ave., University of Wisconsin, Madison, WI 53705. Phone: (608) 262-9708. Fax: (608) 265-2904. E-mail: fox@enzyme.wisc.edu. Mailing address for Glenn H. Chambliss: Department of Bacteriology, Rm. 225 E. B. Fred Hall, University of Wisconsin, Madison, WI 53706. Phone: (608) 262-1161. Fax: (608) 262-9865. E-mail: ghchambl@facstaff.wisc.edu.

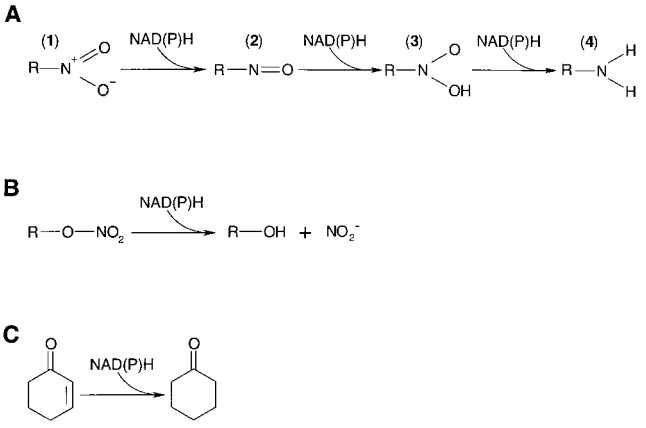

FIG. 1. Representative reduction reactions. (A) Two-electron reduction of an aromatic nitro group by a type I nitroreductase; (B) denitration of a nitroester compound by a xenobiotic reductase; (C) reduction of the α, β-unsaturated bond of 2-cyclohexen-1-one by a xenobiotic reductase.

I-C, respectively, which encode nitroester reductases that denitrate NG (5) and reduce TNT and 2-cyclohexen-1-one.

MATERIALS AND METHODS

Bacterial strains, growth conditions, and plasmids. *P. putida* II-B (5) and *Escherichia coli* DH5α (34) were grown aerobically in Luria-Bertani (LB) medium at 37°C. *P. fluorescens* I-C (5) was incubated aerobically in LB medium at 30°C. Plasmid pUC18 (34) was used for cloning purposes. Cosmid pRK7813 (17) was used for genomic library construction.

Nucleic acid isolation. Genomic DNA was purified by using Puregene reagents (Gentra Systems, Inc., Minneapolis, Minn.). Plasmid DNA was isolated by using the Wizard Plus Minipreps DNA purification system (Promega, Madison, Wis.). Total cellular RNA was isolated by using RNeasy Minipreps (Qiagen, Valencia, Calif.).

Electrophoresis methods. Protein samples were resolved by denaturing gel electrophoresis in 10% polyacrylamide resolving gels, using a Tris-glycine-sodium dodecyl sulfate (SDS) buffer system with β-mercaptoethanol as a reducing agent (22). Proteins were visualized by staining with Coomassie brilliant blue R-250. DNA was visualized on ethidium bromide-stained agarose gels.

Protein characterizations. Protein concentrations were determined by the Bio-Rad (Hercules, Calif.) protein assay, with bovine serum albumin as the standard. The amino-terminal sequence of the purified *P. putida* reductase was determined by automated Edman degradation at the Michigan State University Macromolecular Structure Facility. The amino-terminal sequence of the *P. fluorescens* reductase was determined at the Protein/Nucleic Acid Shared Facility at the Medical College of Wisconsin, Milwaukee. Electrospray ionization mass spectral analysis of the *P. putida* enzyme was conducted at the University of Wisconsin—Madison Biotechnology Center.

DNA sequencing. Sequencing reactions for inclusion as markers on primer extension gels were generated from double-stranded plasmid DNA containing the *xenA* or *xenB* gene by using the T7 Sequenase 2 kit (Amersham Life Science, Arlington Heights, Ill.) and [^{35}S]dATP. All other sequencing reactions were conducted by ABI PRISM (Foster City, Calif.) dye terminator cycle sequencing. The *xenA* and *xenB* gene sequences were determined by a primer walking strategy.

5′ labeling of oligonucleotides. Oligonucleotides used as probes or in primer extension analysis were 5′ labeled with [γ-^{32}P]ATP, using T4 polynucleotide kinase (Gibco BRL, Gaithersburg, Md.). After incubation at 37°C for 30 min, the reactions were stopped by addition of 5 μl of 0.5 M EDTA (pH 8.0). Unincorporated nucleotides were removed from the labeled oligonucleotides with an Auto-Seq G-50 column (Pharmacia Biotech, Piscataway, N.J.).

Genomic library construction. Genomic DNA from *P. putida* and *P. fluorescens* was partially digested with *Sau*3A to generate fragments of 20 to 40 kb. These genomic *Sau*3A fragments were ligated into the *Bam*HI site of pRK7813, packaged by using the Gigapack IIXL (Stratagene, La Jolla, Calif.) packaging system, and transduced into *E. coli* DH5α. Genomic libraries consisting of approximately 1,500 *E. coli* DH5α subclones each were generated for *P. putida* and *P. fluorescens* and maintained on LB medium containing 15 μg of tetracycline per ml.

Genomic library screening. The *P. putida* genomic DNA library was screened using [γ-^{32}P]ATP-labeled degenerate nonoverlapping oligonucleotides designed to be complementary to the amino-terminal sequence of the *P. putida* xenobiotic reductase: 5′-CAR TAY ATG GCS GAR GAC GGI YTG AT-3′ and 5′-TTC GAR CCI TAY ACC YTG AAG GAY GTI AC-3′ (where R = A or G, Y = C or T, S = G or C, and I = inosine). The probes were hybridized to DNA isolated from mixed cultures of library subclones (9). Five-milliliter aliquots of LB medium supplemented with tetracycline (15 μg/ml) were inoculated with 10 *E. coli* DH5α genomic library subclones each and incubated overnight. Cosmid DNA was isolated from these mixed cultures, digested with *Eco*RI and *Hin*dIII, and resolved on 0.7% agarose gels before transfer onto Magnacharge nylon membranes (MSI, Inc., Westboro, Mass.) by Southern blotting. Hybridization was carried out at 42°C in 6× SSPE (1× SSPE is 0.18 M NaCl, 10 mM NaH_2PO_4, and 1 mM EDTA [pH 7.7]) 5× Denhardt's solution, 0.5% SDS, and 100 μg of sonicated and denatured salmon sperm per ml. The membranes were washed in 1× SSPE–0.1% SDS at hybridization temperature prior to analysis with a Molecular Dynamics (Sunnyvale, Calif.) Storm 860 phosphorimaging system. Southern blots were stripped by incubation in 50% formamide–6× SSPE for 30 min at 65°C. Stripped blots were then hybridized to the second oligonucleotide probe, as described above, and phosphor images were compared to identify DNA fragments that hybridized to both oligonucleotide probes. The colonies comprising a mixed culture containing a DNA fragment that hybridized to both probes were then screened individually until a single genomic library subclone was identified.

The *P. fluorescens* genomic DNA library was screened by a colorimetric procedure. Individual *E. coli* DH5α genomic library subclones were inoculated in microtiter plate wells containing 200 μl of LB medium supplemented with tetracycline (15 μg/ml) and incubated overnight. Following incubation, 100 μl of 0.56 mM TNT solution was added to each well and allowed to stand at room temperature for 5 min. Wells were visually screened for library subclones that transformed TNT to a red hydride-Meisenheimer intermediate (39) as described in Results.

Analysis of NG denitration by *P. putida*, *P. fluorescens*, and the *E. coli* DH5α subclones. Starter cultures grown in LB liquid medium were used to inoculate duplicate flasks containing LB medium supplemented with 0.9 mM NG and 100 μg of ampicillin per ml for plasmid selection. Culture density and NG denitration were measured initially and over a 5.5-h period with a Klett-Summerson (New York, N.Y.) photoelectric colorimeter with a red filter and by high-pressure liquid chromatography as previously described (5), respectively. In vitro NG reductase activity was monitored by measuring the rate of NADPH oxidation at 340 nm in the presence of enzyme and NG. The assay buffer was 100 mM potassium phosphate (pH 7.0). A typical assay initially contained 300 μM NG and 130 μM NADPH in 1 ml of assay buffer. Reactions were initiated by the addition of enzyme and monitored for 1 min. One unit of enzyme activity was defined as the oxidation of 1 μmol of NADPH per min at room temperature in the assay buffer, after correction for background NADPH oxidation in the absence of NG.

Analysis of 2-cyclohexen-1-one reduction products. 2-Cyclohexen-1-one, cyclohexanone, and 2-cyclohexen-1-ol were identified by using a Hewlett-Packard model 6890 gas chromatograph (Wilmington, Del.) equipped with a flame ionization detector. The column used was a 15-m by 0.53-mm SE-30 capillary with a film thickness of 1.2 μm (Alltech, Deerfield, Ill.). The injector temperature was 250°C, and the oven temperature was 65°C. Helium was used as a carrier gas at a flow rate of 4.0 ml/min.

RNA primer extension. Primer extension analysis was conducted with total cellular RNA and 0.4 pmol of labeled primer (≈10^5 cpm), 5′-GAA TGG CGA TGC GGT TGC-3′ for *xenA* and 5′-GCC ATG ATG ATG CGG TTG G-3′ for *xenB*, as previously described (40).

To determine whether transcription of a *xenA*-specific message was induced by the presence of NG, *P. putida* and the *E. coli* subclone were grown in LB medium with and without 0.9 mM NG. Cells were harvested in mid-log phase, and total cellular RNA was isolated from each culture. RNA concentrations were determined spectrophotometrically and confirmed by visualization on ethidium bromide-stained agarose gels. To ensure that reverse transcription reactions were not template limited, primer extension analysis was conducted with 2, 4, 6, and 10 μg of RNA. Extension products were quantitated by phosphorimager analysis, and relative levels of extension product were compared to ensure that product levels increased linearly with RNA concentration. Primer extension reactions were conducted in duplicate at each of two independent times, and the averaged results were reported as relative transcription units after normalizing all primer extension product signals in a data set to the intensity of the strongest signal in the data set. A quantitative analysis of *P. fluorescens xenB* transcription was not conducted.

Database searches and sequence alignments. Database searches were performed using the BLAST server from the National Center for Biotechnology Information (NCBI) (2, 29a). Parameters used were the blastx defaults: nr database and filtered query sequence. Pairwise sequence alignments to identify percent identity and percent similarity between sequences were performed by using the NCBI BLAST2 sequences option (29b). Parameters used were the blastp defaults: BLOSUM62 matrix, open gap penalty of 11, extension penalty of 1, gap × dropoff of 50, expect threshold of 10, and filtered query sequence. Amino acid sequences were aligned using the PILEUP program of the Genetics Computer Group (Madison, Wis.). Parameters used were BLOSUM62 matrix, gap penalty of 12, extension penalty of 4, and no penalty for endgaps. Codon usage and GC content data were obtained from Codon Usage Tabulated from GenBank (7a).

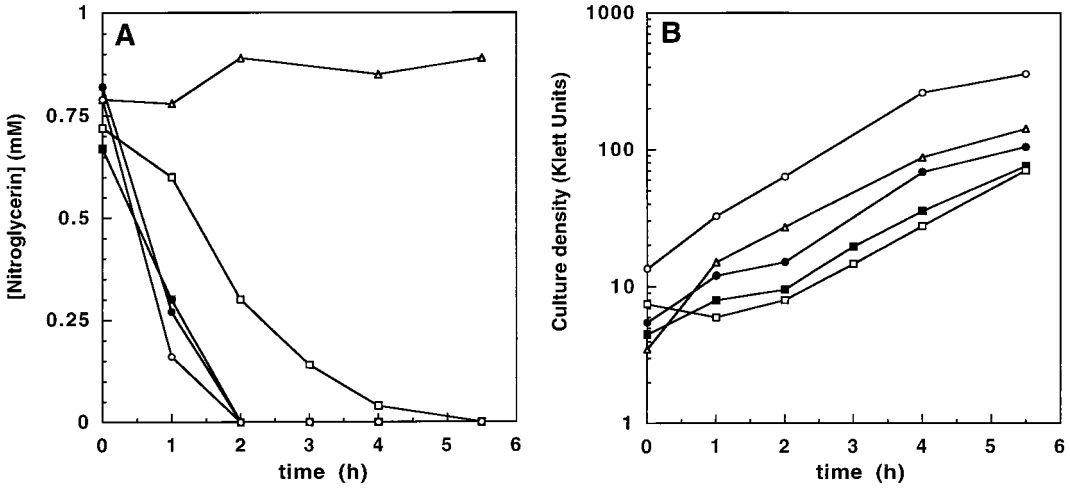

FIG. 2. (A) Time course of the denitration of 0.9 mM NG; (B) time course of the culture density of *P. putida* (○), the *xenA E. coli* DH5α subclone (●), *P. fluorescens* (□), the *xenB E. coli* DH5α subclone (■), and *E. coli* DH5α harboring pUC18 without an insert (△). *P. fluorescens* was incubated at 30°C; all others were incubated at 37°C.

Nucleotide sequence accession number. The nucleotide sequences of *xenA* and *xenB* have been deposited in GenBank under accession no. AF154061 and AF154062, respectively.

RESULTS

Identification and subcloning of the *P. putida* xenobiotic reductase gene, *xenA*. We screened a genomic library of DNA from *P. putida* II-B in pRK7813 by Southern hybridization using degenerate oligonucleotide probes and identified a putative xenobiotic reductase-containing cosmid harboring an approximately 4.3 kb *Acc*I fragment that hybridized to both probes. This fragment was subcloned into pUC18, transformed into *E. coli* DH5α (15), and sequenced. Transformants denitrated NG (Fig. 2A) and grew (Fig. 2B) at rates equivalent to rates for *P. putida*. A 1,092-nucleotide open reading frame (ORF; Fig. 3A), designated *xenA*, was identified within the 4.3-kb subclone. The amino acid sequence deduced from the nucleotide sequence at the 5′ end of *xenA* matched the amino terminus of the purified enzyme determined by Edman degradation, SALFEPYTLKDVTLRNRIAIPPMXQYMAEDGLI NDXHQ (where X = unknown). After removal of the amino-terminal methionine, the predicted molecular weight of the deduced translation product of the *xenA* ORF was 39,702, in close agreement with the M_r of 39,704 determined by electrospray mass spectroscopy after release of FMN from the protein by acid denaturation.

Identification and subcloning of the *P. fluorescens* xenobiotic reductase gene, *xenB*. We observed that the purified *P. fluorescens* xenobiotic reductase transforms TNT (19) to produce a red hydride-Meisenheimer intermediate (λ_{max} = 477 nm [39]). Thus, *E. coli* DH5α genomic library transformants were screened for the ability to produce this red compound in the presence of TNT. A positive clone harboring an approximately 2.2-kb *Hin*dIII fragment of *P. fluorescens* I-C DNA was identified. This fragment was subcloned into pUC18, introduced into *E. coli* DH5α (15), and sequenced. Transformants denitrated NG (Fig. 2A) and grew at rates comparable to those for *P. fluorescens* (Fig. 2B). A 1,050-nucleotide ORF (Fig. 3B), designated *xenB*, was identified within the subcloned fragment. The amino acid sequence deduced from the nucleotide sequence at the 5′ end of *xenB* matched the amino terminus of the purified enzyme determined by Edman degradation, ATIFDPIKLGDIELSNRI. After removal of the amino-terminal methionine, the predicted molecular weight of the deduced translation product of the *xenB* ORF was 37,441, in close agreement with the native M_r of 37,000 determined by sedimentation velocity measurements (5).

Features of the *xenA* and *xenB* ORFs and flanking DNA. The *xenA* and *xenB* ORFs have 66 and 64% GC content, respectively, values close to the 60% overall GC content observed for *P. putida* and *P. fluorescens*. A 26-bp region exhibiting dyad symmetry, followed immediately by four adenine nucleotides, characteristic of a rho-independent transcriptional terminator (6, 7), is situated three nucleotides downstream from the *P. putida xen*A stop codon (Fig. 3A). A similar 28-bp region is located 28 nucleotides downstream of the *P. fluorescens xen*B stop codon (Fig. 3B).

Analysis of the cloned DNA sequence flanking the *P. putida xen*A gene revealed several ORFs with deduced amino acid sequences similar to those of previously identified proteins (Fig. 4A). The amino acid sequence encoded by partial ORF1 (>1,585 nucleotides) exhibits 64% identity and 76% similarity to a putative *E. coli* malate, quinone flavoprotein oxidoreductase (accession no. P33940). ORF2 (300 nucleotides) is a complete coding region, with in-frame translational start and stop codons, encoding a putative protein with 45% amino acid identity and 61% amino acid similarity to a putative *B. subtilis* transcriptional regulator, YczG (accession no. Z99106.1), belonging to the *arsR* family of transcriptional regulators for enzymes that reduce arsenate to arsenite (46). Region 3 (1,145 nucleotides), downstream of *P. putida xenA*, exhibits 88% nucleotide identity to 1,145 bases of uncharacterized DNA downstream of the *P. putida* α-ketoglutarate semialdehyde dehydrogenase gene (accession no. M69158). Within region 3, a deduced stretch of 176 amino acids shows 28% identity and 49% similarity to amino acids 39 to 219 of a putative flavoprotein, D-amino acid dehydrogenase from *Halorhodospira halophila* (accession no. P42515), which may be involved in alanine catabolism (3, 16).

The DNA sequence flanking the *xenB* gene contains two partial ORFs with deduced amino acid sequences similar to those of previously identified proteins (Fig. 4B). Partial ORF4 (>303 nucleotides), upstream of the *xenB* gene, encodes a sequence with 51% amino acid identity and 68% amino acid

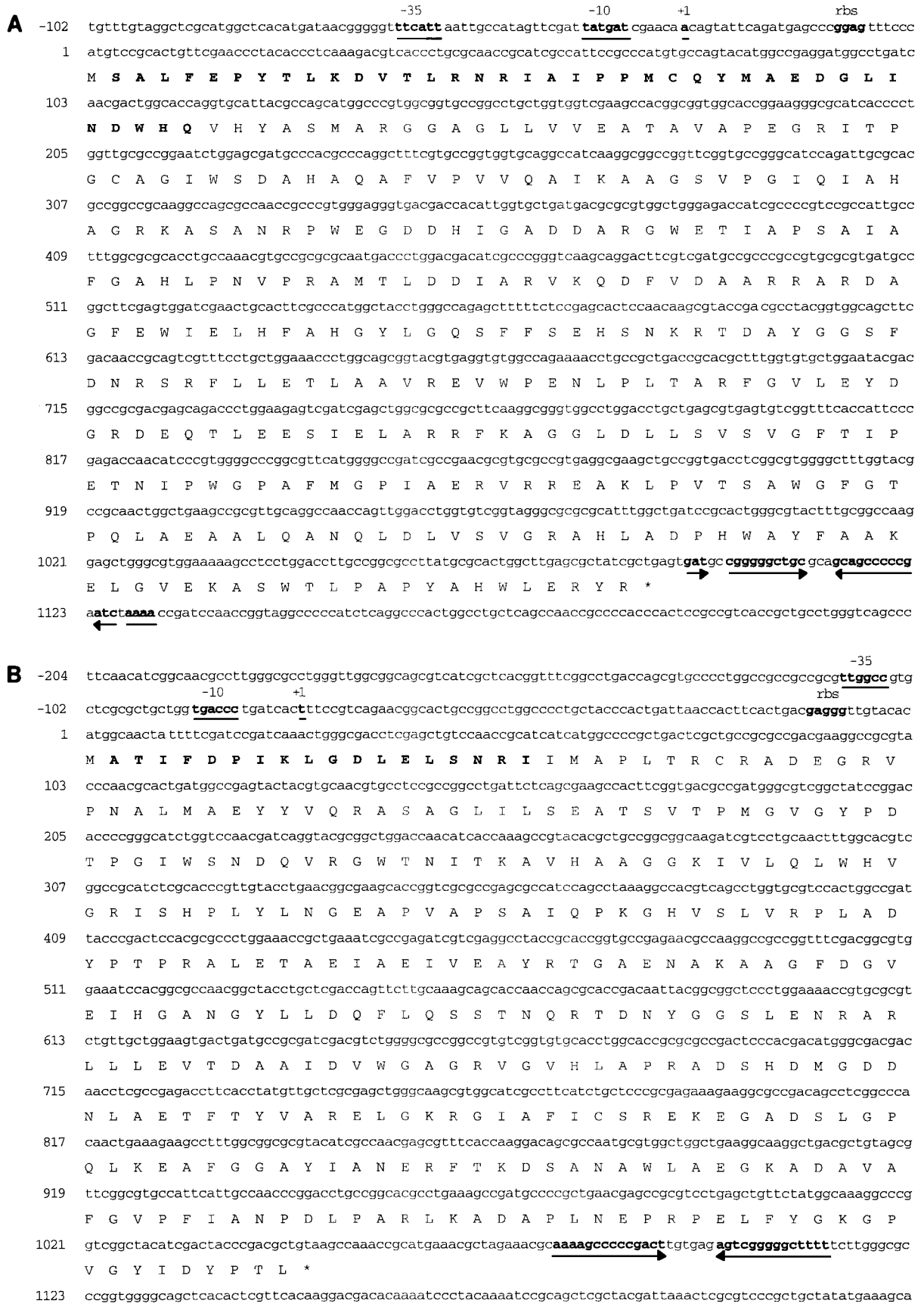

FIG. 3. Complete nucleotide sequence and deduced amino acid sequence of the *P. putida xenA* gene (A) and the *P. fluorescens xenB* gene (B). Amino acid residues that correspond to the amino-terminal sequences determined by Edman degradation are shown in boldface type; putative −10 and −35 promoter elements and ribosome-binding sites (rbs) as well as the transcription initiation sites (+1) identified by primer extension are indicated. Inverted repeats downstream of the stop codons are denoted with arrowheads; four adenines following the *xenA* inverted repeat are underlined.

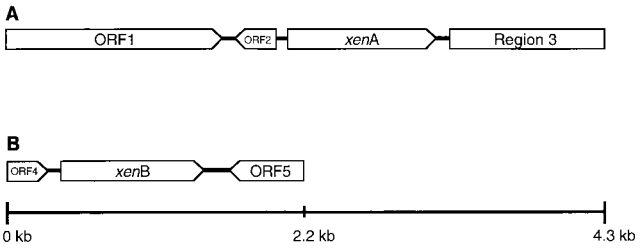

FIG. 4. Linear maps of putative coding regions flanking *P. putida xenA* (A) and *P. fluorescens xenB* (B). Proposed direction of transcription is shown by the arrowhead at the end of each indicated coding region. The identity of each proposed ORF is reported in Results as the top hit from a BLAST search conducted by using the deduced amino acid sequence of each indicated ORF.

similarity to AraJ of *E. coli* (accession no. AAC74729), a putative transport protein that may serve a role in arabinose utilization and is also related to a *Streptomyces* chloramphenicol resistance protein (29). Partial ORF5 (>543 nucleotides), downstream of the *xen*B gene, encodes a sequence with 42% amino acid identity and 59% amino acid similarity to the putative *E. coli* transcriptional repressor AcrR (accession no. P34000), which may regulate multidrug efflux pumps that confer resistance to acriflavine and other hydrophobic antibiotics in *E. coli* (23, 24).

Expression of recombinant *xenA* and *xenB* in *E. coli*. SDS-polyacrylamide gel electrophoresis analysis indicated that *xenA* and *xenB* were highly expressed in the *E. coli* DH5α subclones (Fig. 5). Cell extracts of *P. putida*, *P. fluorescens*, and the *E. coli* subclones exhibited prominent protein bands that comigrated with pure xenobiotic reductase protein from either *P. putida* or *P. fluorescens*. In contrast, lysates from *E. coli* DH5α harboring the plasmid pUC18 lacking a DNA insert did not exhibit protein bands that comigrated with XenA or XenB. In vitro activity assays conducted with cell extract confirmed that the

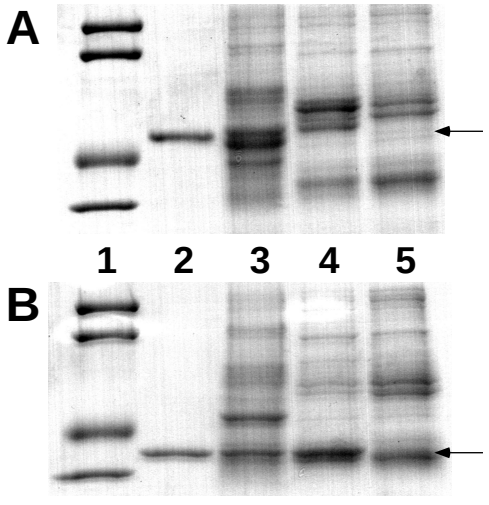

FIG. 5. Denaturing gel electrophoresis analysis. (A) Comparison of 1 μg of xenobiotic reductase purified from *P. putida* (lane 2) to approximately 20 μg of cell extract from *P. putida* (lane 3), *E. coli* DH5α *xenA* subclone (lane 4), and *E. coli* DH5α harboring plasmid pUC18 lacking a DNA insert (lane 5); (B) comparison of 1 μg of xenobiotic reductase purified from *P. fluorescens* (lane 2) to approximately 20 μg of cell extract from *P. fluorescens* (lane 3), *E. coli* DH5α *xenB* subclone (lane 4), and *E. coli* DH5α harboring plasmid pUC18 lacking a DNA insert (lane 5). An arrow indicates the protein band that corresponds to the xenobiotic reductase enzyme expressed by each *E. coli* subclone in lanes 4. Lanes 1, molecular mass standards of 94, 67, 43, and 30 kDa.

TABLE 1. NG reductase specific activity of cell extracts

Cell extract	Sp act (U/mg)[a]
P. putida	0.4
E. coli DH5α/pUC18 *xenA* subclone	0.6
P. fluorescens	0.4
E. coli DH5α/pUC18 *xenB* subclone	0.8
E. coli DH5α/pUC18	0.001

[a] One unit of activity is defined as the oxidation of 1 μmol of NADPH per min in the presence of 300 μM NG in 100 mM potassium phosphate buffer (pH 7.0) at room temperature.

expressed proteins had catalytic activity and exhibited over 500-fold-greater specific activity than cell extracts from *E. coli* DH5α harboring the plasmid pUC18 lacking an insert (Table 1).

Substrate specificity of the xenobiotic reductases. Table 2 shows a comparison of the substrate specificities of purified xenobiotic reductases from *P. putida* and *P. fluorescens*. Both enzymes exhibited the greatest rates of NADPH oxidation when NG was provided as an electron acceptor, although TNT and 2-cyclohexen-1-one could be reduced to various degrees. The *P. fluorescens* oxidoreductase exhibited fivefold-greater activity with TNT than did the *P. putida* enzyme. Conversely, the *P. putida* oxidoreductase exhibited approximately sevenfold-greater activity with 2-cyclohexen-1-one than did the *P. fluorescens* enzyme.

Gas chromatographic analysis of 2-cyclohexen-1-one degradation products showed that both enzymes reduced the double bond of the hexene to produce cyclohexanone; no 2-cyclohexen-1-ol was detected. This product distribution is similar to that observed from the *P. syringae* pv. glycinea flavoprotein oxidoreductase Ncr (32).

As exemplified by a low rate of NADPH oxidation in the presence of TNT, *P. putida* XenA transformed TNT slowly. In contrast, *P. fluorescens* XenB rapidly transformed TNT. An analysis of the products of TNT transformation by the *P. fluorescens* oxidoreductase will be reported elsewhere (19).

RNA primer extension analysis of *xenA* and *xenB*. RNA primer extension analysis was performed to map the transcription initiation site of *xenA* in both *P. putida* and the *E. coli* DH5α subclone. In both organisms, the *xenA* transcription start site was found to be the adenine located 29 nucleotides upstream from the ATG translation initiation codon (Fig. 6A). A putative −10 hexamer (TATGAT) is located 6 nucleotides upstream of the transcription initiation site, and a possible −35 hexamer (TTCATT) is located 17 nucleotides upstream of the −10 hexamer (Fig. 3A).

TABLE 2. Specific activities of purified xenobiotic reductases from *P. putida* and *P. fluorescens* with several substrates

Substrate	Sp act (U/mg)[a]
P. putida	
NG	6.1
TNT	0.5
2-Cyclohexen-1-one	4.1
P. fluorescens	
NG	6.8
TNT	2.5
2-Cyclohexen-1-one	0.6

[a] One unit of activity is defined as the oxidation of 1 μmol of NADPH per min in the presence of 300 μM NG, TNT, or 2-cyclohexen-1-one in 100 mM potassium phosphate buffer (pH 7.0) at room temperature.

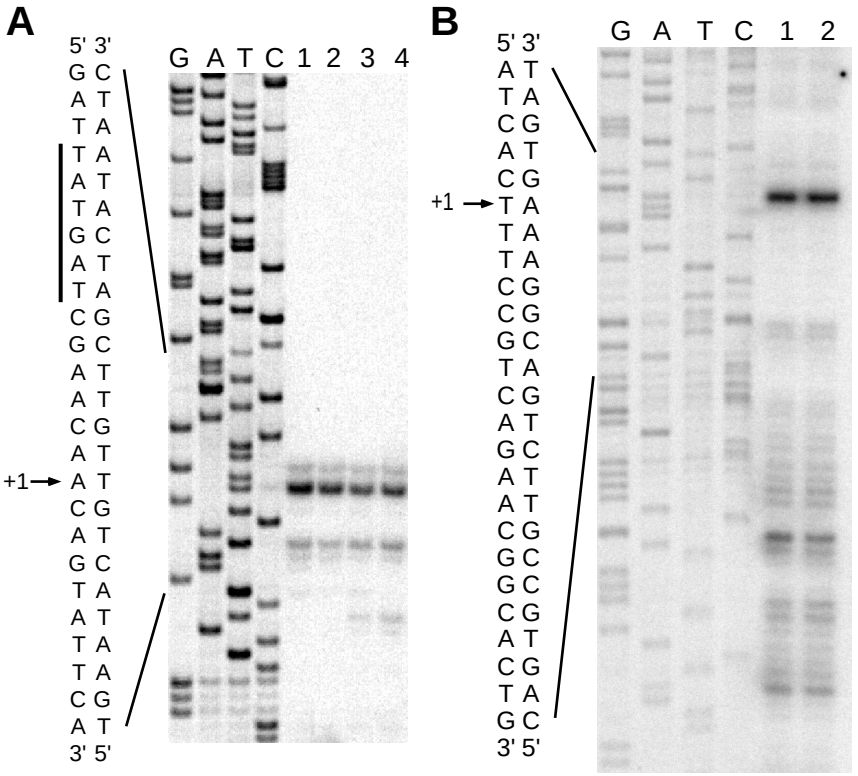

FIG. 6. Primer extension mapping of the *xenA* (A) and *xenB* (B) transcriptional start sites. cDNA from reverse transcription reactions was loaded onto sequencing gels next to sequencing reactions (lanes GATC) conducted with the same primer. (A) Products from reactions containing 10 μg of *P. putida* or *E. coli xenA* subclone RNA are shown in lanes 1 to 4. Total RNA was isolated from *P. putida* (lanes 1 and 2) and from the *E. coli* subclone (lanes 3 and 4) after growth in LB medium (lanes 1 and 3) or LB medium supplemented with 0.9 mM NG (lanes 2 and 4). An expanded view of the nucleotide sequence surrounding the transcription initiation site (+1) is shown, and the putative −10 hexamer is highlighted with a vertical bar. (B) cDNA products from reactions containing 2 μg of *E. coli xenB* subclone RNA are shown in lanes 1 and 2. The nucleotide sequence surrounding the transcription initiation site (+1) is shown.

Primer extension mapping of the *P. fluorescens xenB* transcription start site was also conducted and revealed a probable *xenB* transcriptional start site in *E. coli* DH5α at the thymine located 75 nucleotides upstream from the ATG translational initiation codon (Fig. 6B). Primer extension analysis using total RNA isolated from *P. fluorescens* also exhibited a band consistent with initiation at the same thymine identified in the *E. coli* subclone (data not shown). A potential −10 hexamer (TG ACCC) lies 7 nucleotides upstream of the *xen*B transcription initiation site, with a putative −35 hexamer (TTGGCC) spaced 16 nucleotides upstream of the −10 hexamer (Fig. 3B).

***xenA* message quantitation by RNA primer extension.** The amount of *xenA*-specific message produced by *P. putida* and the *E. coli* subclone was measured from cells grown in medium with and without NG. The relative amounts of *xenA* transcripts remained constant in *P. putida* and *E. coli*, regardless of whether NG was included in the medium (Table 3). Also, relative *xenA* transcript levels were similar in the homologous host strain, *P. putida*, and the heterologous *E. coli* DH5α subclone. Due to difficulties in isolating intact RNA from *P. fluorescens*, a similar expression analysis was not conducted with *xenB*.

Database comparisons and sequence analysis. The deduced amino acid sequences of the *P. putida* and the *P. fluorescens* xenobiotic reductases were compared with sequences in GenBank, using the NCBI BLASTP program. Several bacterial flavoproteins were identified, including *Agrobacterium radiobacter* glycerol trinitrate (GTN) reductase (accession no. CAA74280; 31% identity and 50% similarity to XenA; 49% identity and 62% similarity to XenB), *Enterobacter cloacae* PETN reductase (accession no. AAB38683; 29% identity and 44% similarity to XenA; 47% identity and 61% similarity to XenB), *E. coli N*-ethylmaleimide reductase (accession no. P77258; 28% identity and 44% similarity to XenA; 47% identity and 60% similarity to XenB), *P. syringae* 2-cyclohexen-1-one reductase (accession no. AF093246; 30% identity and 47% similarity to XenA; 48% identity and 62% similarity to XenB), *P. putida* M10 morphinone reductase (accession no. 564687; 29% identity and 47% similarity to XenA; 50% identity and 61% similarity to XenB), several homologs of yeast OYE (28% identity and 46% similarity to XenA; 35% identity and 48%

TABLE 3. Relative levels of the extended cDNA products from primer extension reactions

Concn (mM) of NG in growth medium	Relative transcription units[a] ± SD
P. putida	
0	0.7 ± 0.3
0.9	0.5 ± 0.2
E. coli xenA subclone	
0	0.5 ± 0.2
0.9	0.7 ± 0.2

[a] Defined as the intensity of reverse transcription bands as quantitated by phosphorimaging. The reported values were normalized to the intensity of the strongest signal observed in the reaction set.

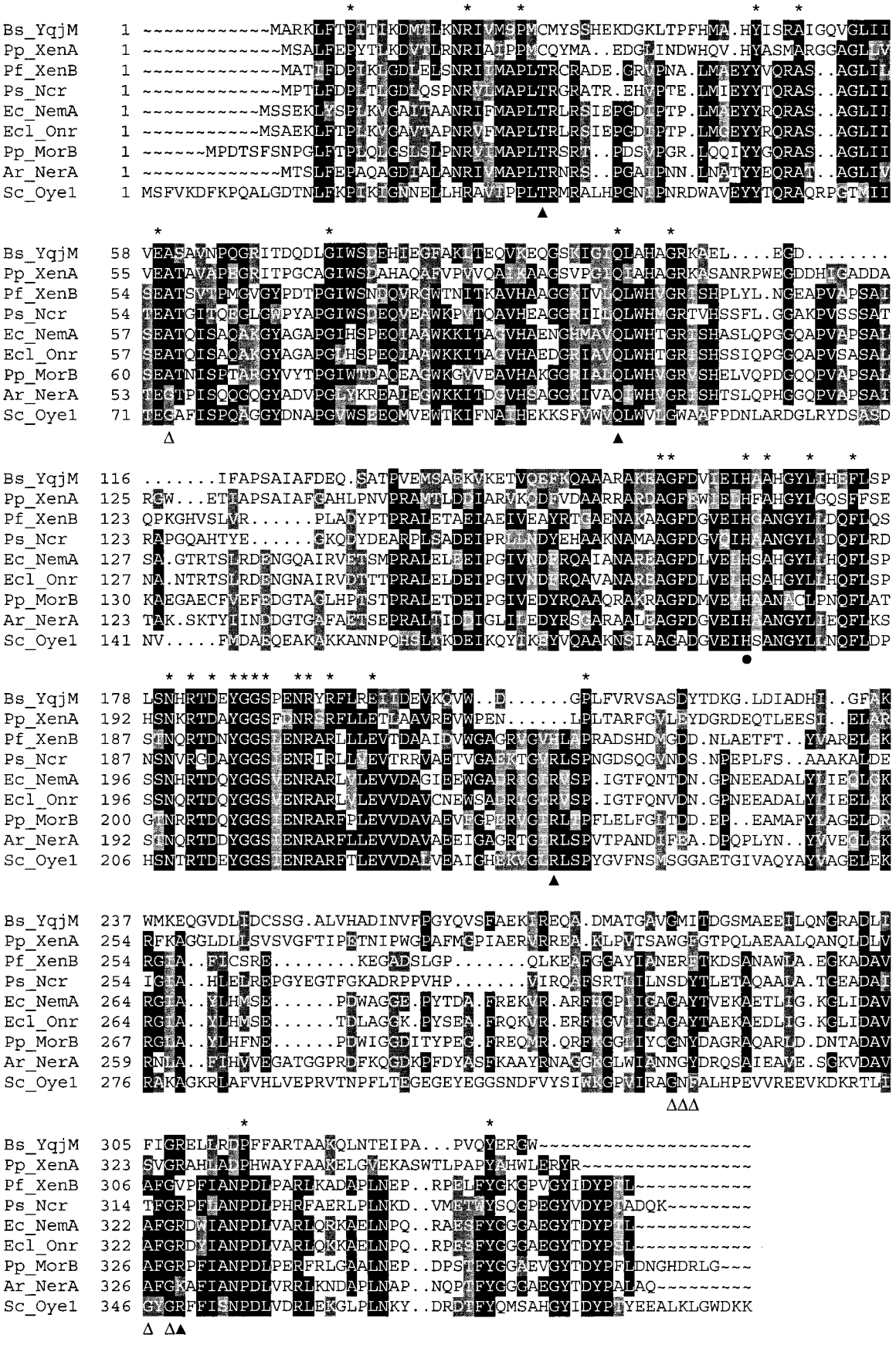

similarity to XenB for OYE isoform 1 from *Saccharomyces carlsbergensis* [accession no. X53597]), and a hypothetical *Bacillus subtilis* protein, YqjM (accession no. P54550; 40% identity and 54% similarity to XenA; 38% identity and 54% similarity to XenB).

Figure 7 shows an alignment of deduced amino acid sequences of the *P. putida* and *P. fluorescens* xenobiotic reductases with the amino acid sequences of PETN reductase, GTN reductase, *N*-ethylmaleimide reductase, 2-cyclohexen-1-one reductase, morphinone reductase, *B. subtilis* YqjM, and *S. carlsbergensis* OYE. Excluding uncharacterized *B. subtilis* YqjM, the amino acid sequences aligned in Fig. 7 exhibit an average of 46% identity and 59% similarity in comparison to the *P. fluorescens* reductase, whereas they possess an average of 29% identity and 46% similarity in comparison to the *P. putida* reductase. Compared to each other, the deduced amino acid sequences of XenA and XenB show 34% identity and 51% similarity. In contrast, certain other protein sequences within this enzyme family, such as *E. coli N*-ethylmaleimide reductase and *E. cloacae* PETN reductase (87% identity; 93% similarity), are much more closely related. *P. putida* XenA is most closely related to *B. subtilis* YqjM, while *P. fluorescens* XenB is more similar to the other amino acid sequences included in the alignment (Fig. 7).

Amino acid sequence alignments reveal that functionally important residues comprising the FMN-binding site and active site of OYE from *S. carlsbergensis* are conserved among the compared proteins (Fig. 7). Ten residues that form hydrogen bonds to the FMN prosthetic group in OYE have been identified (11). In the nine proteins compared in Fig. 7, 2 of 10 residues implicated in flavin binding by OYE (Gln-114 and Gly-347) are conserved in all nine sequences compared, and 6 additional residues from OYE implicated in flavin binding (Thr-37, Gly-72, Arg-243, Phe-326, Gly-345, and Arg-348) are maintained or conservatively substituted in seven to nine of the sequences compared. Additionally, active-site residue His-191 of OYE is conserved among all nine proteins. Interestingly, active-site residue Asn-194 of OYE is conserved in *P. putida* morphinone reductase, *A. radiobacter* GTN reductase, *P. syringae* cyclohexen-1-one reductase, and the *P. fluorescens* xenobiotic reductase but substituted by His in the other four proteins compared in Fig. 7. Previously, Karplus et al. observed that Asn-194 of OYE was also substituted by His in members of an additional group of α/β-barrel flavoproteins that possess accessory domains fused to their amino or carboxy termini, including trimethylamine dehydrogenase, NADH oxidase, and bile acid-inducible proteins C and H (18). The effect of this substitution on catalysis is unknown. Further, a 21-amino-acid stretch spanning from Ser-207 to Glu-227 in OYE is well conserved among all of the proteins compared. In OYE, residues in this region form a helix that interacts with its symmetry mate across the dimer interface. Additional functional roles for these residues are unclear (11).

DISCUSSION

An examination of amino acid sequence and biochemical properties confirms that the *P. putida* and *P. fluorescens* xenobiotic reductases belong to a bacterial subgroup of a family of α/β-barrel flavoprotein oxidoreductases exemplified by yeast OYE. Members of this protein family have a subunit size of approximately 40 kDa, contain FMN, and utilize NAD(P)H as a reductant. Although OYE has been well characterized, its physiological function remains unknown (18). Similarly, the bacterial members of this protein family catalyze redox reactions with diverse electrophilic xenobiotic substrates but share no known physiological substrate.

Heterologous expression of *xenA* and *xenB* in *E. coli* DH5α. The *E. coli* subclones expressed *xenA* and *xenB* without the aid of a plasmid-encoded expression promoter, suggesting that transcription was driven by a native promoter contained within the cloned inserts. Primer extension analysis revealed that the transcription initiation sites of *xenA* in *P. putida* and in the heterologous host *E. coli* DH5α were the same (Fig. 6A), confirming that *xenA* was transcribed from its *Pseudomonas* promoter in *E. coli*. The cloned xenobiotic reductases expressed in *E. coli* DH5α exhibited levels of NG reduction equivalent to those for the homologous *Pseudomonas* host strains (Fig. 2A; Table 1). However, as the *E. coli* subclones harbor the xenobiotic reductase genes on the multicopy plasmid pUC18, *xenA* and *xenB* presumably are not expressed as efficiently in *E. coli* as in *Pseudomonas* species.

P. putida produces a large amount of XenA, approximately 16% of the soluble protein in the cell (5). One reason for this high protein level may be a strong promoter, as indicated by the similarity between the proposed *xenA* promoter elements (Fig. 3A) and the consensus *E. coli* $E\sigma^{70}$ promoter. The putative −10 hexamer varied at one position from the $E\sigma^{70}$ consensus (TATAAT), while the −35 hexamer differed at three positions from consensus (TTGACA) [30]). The spacer regions between the −35 and −10 hexamers, and between the −10 hexamer and the transcription initiation site, were consensus distances for an $E\sigma^{70}$ promoter (30). As reviewed by Record et al., variation of promoter elements from the consensus, as observed with the proposed *xenA* promoter, may actually serve to increase promoter strength, as a promoter identical to the $E\sigma^{70}$ consensus may bind RNA polymerase too tightly, preventing formation of an elongating complex (30). Additional inspection of the *xenA* promoter region did not reveal other obvious features that might contribute to increased promoter strength, such as an UP element or an extended −10 region (10, 30). Other mechanisms contributing to natural hyperexpression of *xenA* are under investigation.

P. fluorescens also produces a large amount of XenB (5); however, the proposed promoter elements upstream of the *xenB* transcriptional start site (Fig. 3B) did not match the *E. coli* $E\sigma^{70}$ consensus as closely as the putative *xenA* promoter elements (Fig. 3A). As *Pseudomonas* promoters are not well characterized, the *xenB* promoter may be recognized by a sigma factor that binds sequence elements that differ from the $E\sigma^{70}$ consensus.

Comparison of the xenobiotic reductases to nitroreductases. The *P. putida* and *P. fluorescens* xenobiotic reductases, the other related xenobiotic reductases, and the oxygen-insensitive type I nitroreductases are broad-specificity, FMN-containing flavoproteins that reduce nitro-substituted compounds by us-

FIG. 7. Alignment of the deduced amino acid sequences of *B. subtilis* YqjM (Bs_YqjM), *P. putida* xenobiotic reductase XenA (Pp_XenA), *P. fluorescens* xenobiotic reductase XenB (Pf_XenB), *P. syringae* 2-cyclohexen-1-one reductase Ncr (Ps_Ncr), *E. coli N*-ethylmaleimide reductase NemA (Ec_NemA), *E. cloacae* PETN reductase Onr (Ecl_Onr), *P. putida* morphinone reductase MorB (Pp_MorB), *A. radiobacter* GTN reductase NerA (Ar_NerA), and *S. carlsbergensis* OYE isoform 1 (Sc_Oye1). Consensus of at least 50% identical amino acid residues is denoted by black boxes; conserved amino acid substitutions are highlighted with grey boxes. Amino acid residues conserved in all nine sequences are overmarked with asterisks. ▲, amino acid residues from OYE that form side chain hydrogen bonds with FMN; △, OYE residues that form main chain hydrogen bonds with FMN; ●, OYE active-site residue His-191.

ing NAD(P)H as a reductant. However, amino acid sequence alignments comparing the xenobiotic reductases and the type I nitroreductases do not reveal biologically relevant similarities between these enzyme families.

The amino acid sequence differences are accentuated by structural comparisons of representative enzymes related to the xenobiotic reductases and the nitroreductases. The structure of a xenobiotic reductase has not been reported. However, OYE from *S. carlsbergensis*, which has been structurally defined (11), shows an average of 35% amino acid identity and 50% amino acid similarity with the bacterial xenobiotic reductases. Also, while the structure of a nitroreductase has not been published, X-ray structures for two FMN-containing flavin reductases, flavin reductase P (FRP) of *Vibrio harveyi*, and flavin reductase (FRase) I of *V. fischeri*, are available (21, 38) and reveal a common protein fold (21). FRP and FRase I provide free $FMNH_2$ for bacterial bioluminescence, which is a biological function different from that of the nitroreductases. However, they are related to the nitroreductases in amino acid sequence, and the close evolutionary relationship between the nitroreductases and FMN-containing flavin reductases was demonstrated by showing that nitroreductases NsfA and NsfB could be converted to flavin reductases with activities similar to those of FRP and FRase I, respectively, by single amino acid substitutions (47, 48).

Comparison of the structures of OYE, FRP, and FRase I reveals that OYE differs from the two FMN-containing flavin reductases with respect to the basic protein folds. A structural analysis of OYE revealed that each subunit folds into a single domain, centered around a parallel, eight-stranded α/β-barrel comprised of alternating parallel β-sheets and α-helices (11). In contrast, the FRP and FRase I subunits each fold into two domains. For both flavin reductases, the first domain comprises the core fold, consisting of a four-stranded antiparallel β-sheet that interacts with a fifth, parallel β-strand from the carboxy terminus of the other subunit, flanked by α-helices (21, 38). Thus, structural analysis suggests that FRP and FRase I, as well as related nitroreductases, such as NsfA and NsfB, were likely derived from a common ancestral flavoprotein (21), while OYE and the bacterial xenobiotic reductases, as represented by the α/β-barrel structure of OYE, were likely derived from a different ancestral protein fold.

Physiological role of the xenobiotic reductases. The physiological function of the xenobiotic reductases is unknown; however, genes involved in similar metabolic activities are often arranged together on the bacterial chromosome. The *P. putida* reductase is flanked by two putative metabolic enzymes and by a putative transcriptional regulator of arsenic degradation. The *P. fluorescens* xenobiotic reductase is flanked by partial ORFs that may encode an antibiotic efflux protein and a regulator of antibiotic efflux. Thus, both reductases are flanked by enzymes and/or regulatory proteins that may function in detoxification reactions.

Although OYE was first purified over 65 years ago (42) and seven homologous bacterial flavoproteins have since been characterized, a single class of physiological substrates has not been identified. Rather, these enzymes reduce a variety of electrophilic substrates. Further, the numerous substrates that react with the bacterial xenobiotic reductases do not universally serve as substrates for all seven enzymes. For example, *N*-ethylmaleimide reductase (NemA) of *E. coli* DH5α reduces *N*-ethylmaleimide to *N*-ethylsuccinimide (27). NemA is 87% identical and 93% similar to the *E. cloacae* NG-degrading enzyme PETN reductase. However, we observed that *E. coli* DH5α did not degrade NG (Fig. 2A; Table 1). The fact that Miura et al. purified catalytically active NemA from *E. coli* DH5α (28) indicates that either *E. coli* DH5α does not express *nem*A under the growth conditions used in our laboratory or that NG is not a substrate for NemA.

Additional enzymes related to the xenobiotic reductases likely remain to be discovered in other bacterial species. For example, the *B. subtilis* ORF *yqjM* is identified in GenBank as encoding a probable NADH-dependent flavin oxidoreductase. The putative protein encoded by this ORF is highly similar (54%) to the *P. putida* xenobiotic reductase. Although expression of *yqjM* has not been demonstrated, the ORF is preceded by possible promoter elements that match the *B. subtilis* $E\sigma^A$ consensus at 10 of 12 positions, suggesting that the gene may be expressed (41). In preliminary experiments, *B. subtilis* did not degrade NG (data not shown). Thus, the questions of whether *B. subtilis yqjM* is expressed and, if it is, with what substrates the protein reacts remain to be answered.

Kohli and Massey recently proposed that the physiological oxidant of OYE has not been discovered because such a substrate does not exist (20). Rather, OYE may function along with other constituents of the antioxidant defense systems, including glutathione reductase, superoxide dismutase, catalase, and peroxidase, to protect cells against various toxic compounds. This role for OYE is supported by a study in which DNA microarrays were used to identify genes in *Saccharomyces cerevisiae* for which mRNA levels increased by more than threefold upon overexpression of Yap1, a transcription factor that confers upon yeast increased resistance to environmental stresses (8). Two OYE genes were identified.

OYE and the related bacterial xenobiotic reductases described herein share many biochemical properties and conserved regions of amino acid sequence, which provides evidence that these enzymes form an evolutionarily related family. Based on this relationship, we hypothesize that these prokaryotic enzymes serve a detoxification role in bacteria similar to that proposed for OYE in yeast. Evolutionarily, the xenobiotic reductases may provide a selective advantage to bacteria under various conditions of environmental stress. Further study of these genes may help to reveal factors governing horizontal transfer of genetic information among related bacterial species in the environment. Furthermore, as additional examples of these enzymes are discovered, the list of substrates transformed should continue to grow. This potential provides a rich opportunity to probe the structure-function relationships that determine substrate specificity among this flavoprotein family.

ACKNOWLEDGMENTS

This work was supported by U.S. Army ARDEC contract DAAA21-93-C-1034, the Department of Bacteriology and the College of Agricultural and Life Sciences, University of Wisconsin-Madison, to G.H.C. and National Science Foundation grant MCB-973331 to B.G.F. B.G.F. is a Shaw Scientist of the Milwaukee Foundation, 1994 to 1999.

We thank T. Kinscherf (Department of Plant Pathology, University of Wisconsin—Madison) for providing invaluable technical assistance in constructing the *Pseudomonas* genomic libraries, E. Cahoon (DuPont, Wilmington, Del.) for sequencing the *P. fluorescens xenB* gene, and J. Gralnick (Department of Bacteriology, University of Wisconsin—Madison) for sharing his expertise with the Genetics Computer Group software package.

REFERENCES

1. **Åkeson, Å., A. Ehrenberg, and H. Theorell.** 1963. Old yellow enzyme, p. 339–416. *In* P. D. Boyer, H. Lardy, and K. Myrbäck (ed.), The enzymes. Academic Press, New York, N.Y.
2. **Altschul, S. F., T. L. Madden, A. A. Schaffer, J. Zhang, Z. Zhang, W. Miller, and D. J. Lipman.** 1997. Gapped BLAST and PSI-BLAST: a new generation of protein database search programs. Nucleic Acids Res. **25:**3389–3402.

3. **Baca, M., G. E. Borgstahl, M. Boissinot, P. M. Burke, D. R. Williams, K. A. Slater, and E. D. Getzoff.** 1994. Complete chemical structure of photoactive yellow protein: novel thioester-linked 4-hydroxycinnamyl chromophore and photocycle. Biochemistry **33:**14369–14377.
4. **Binks, P. R., C. E. French, S. Nicklin, and N. C. Bruce.** 1996. Degradation of pentaerythritol tetranitrate by *Enterobacter cloacae* PB2. Appl. Environ. Microbiol. **62:**1214–1219.
5. **Blehert, D. S., K. L. Knoke, B. G. Fox, and G. H. Chambliss.** 1997. Regioselectivity of nitroglycerin denitration by flavoprotein nitroester reductases purified from two *Pseudomonas* species. J. Bacteriol. **179:**6912–6920.
6. **Brendel, V., G. H. Hamm, and E. N. Trifonov.** 1986. Terminators of transcription with RNA polymerase from *Escherichia coli*: what they look like and how to find them. J. Biomol. Struct. Dyn. **3:**705–723.
7. **Carafa, Y. A., E. Brody, and C. Thermes.** 1990. Prediction of rho-independent *Escherichia coli* transcription terminators. J. Mol. Biol. **216:**835–858.

7a. **Codon Usage Database.** 15 August 1998, posting date. Codon Usage Tabulated from GenBank. [Online.] http://www.dna.affrc.go.jp/~nakamura/CUTG.html. [27 August 1999, last date accessed.]

8. **DeRisi, J. L., V. R. Iyer, and P. O. Brown.** 1997. Exploring the metabolic and genetic control of gene expression on a genomic scale. Science **278:**680–686.
9. **Donohue, T. J., A. G. McEwan, and S. Kaplan.** 1986. Cloning, DNA sequence, and expression of the *Rhodobacter sphaeroides* cytochrome c_2 gene. J. Bacteriol. **168:**962–972.
10. **Estrem, S. T., T. Gaal, W. Ross, and R. L. Gourse.** 1998. Identification of an UP element consensus sequence for bacterial promoters. Proc. Natl. Acad. Sci. USA **95:**9761–9766.
11. **Fox, K. M., and P. A. Karplus.** 1994. Old yellow enzyme at 2 Å resolution: overall structure, ligand binding, and comparison with related flavoproteins. Structure **2:**1089–1105.
12. **French, C. E., and N. C. Bruce.** 1994. Purification and characterization of morphinone reductase from *Pseudomonas putida* M10. Biochem. J. **301:**97–103.
13. **French, C. E., S. Nicklin, and N. C. Bruce.** 1998. Aerobic degradation of 2,4,6-trinitrotoluene by *Enterobacter cloacae* PB2 and by pentaerythritol tetranitrate reductase. Appl. Environ. Microbiol. **64:**2864–2868.
14. **Gorontzy, T., O. Drzyzga, M. W. Kahl, D. Bruns-Nagel, J. Breitung, E. von Loew, and K. H. Blotevogel.** 1994. Microbial degradation of explosives and related compounds. Crit. Rev. Microbiol. **20:**265–284.
15. **Hanahan, D.** 1985. Techniques for transformation of *E. coli*, p. 109–135. *In* D. M. Glover (ed.), DNA cloning: a practical approach. IRL Press, Oxford, England.
16. **Janes, B. K., and R. A. Bender.** 1998. Alanine catabolism in *Klebsiella aerogenes*: molecular characterization of the *dadAB* operon and its regulation by the nitrogen assimilation control protein. J. Bacteriol. **180:**563–570.
17. **Jones, J. D. G., and N. Gutterson.** 1987. An efficient mobilizable cosmid vector, pRK7813, and its use in a rapid method for marker exchange in *Pseudomonas fluorescens* strain HV37a. Gene **61:**299–306.
18. **Karplus, A. P., K. M. Fox, and V. Massey.** 1995. Structure-function relations for old yellow enzyme. FASEB J. **9:**1518–1526.
19. **Knoke, K. L., D. R. Noguera, B. G. Fox, and G. H. Chambliss.** Unpublished data.
20. **Kohli, R. M., and V. Massey.** 1998. The oxidative half-reaction of old yellow enzyme. J. Biol. Chem. **273:**32763–32770.
21. **Koike, H., H. Sasaki, T. Kobori, S. Zenno, K. Saigo, M. E. P. Murphy, E. T. Adman, and M. Tanokura.** 1998. 1.8 Å crystal structure of the major NAD(P)H:FMN oxidoreductase of a bioluminescent bacterium, *Vibrio fischeri*: overall structure, cofactor and substrate-analog binding, and comparison with related flavoproteins. J. Mol. Biol. **280:**259–273.
22. **Laemmli, U. K.** 1970. Cleavage of structural proteins during the assembly of the head of bacteriophage T4. Nature **227:**680–685.
23. **Ma, D., M. Alberti, C. Lynch, H. Nikaido, and J. E. Hearst.** 1996. The local repressor AcrR plays a modulating role in the regulation of *acr*AB genes of *Escherichia coli* by global stress signals. Mol. Microbiol. **19:**101–112.
24. **Ma, D., D. N. Cook, M. Alberti, N. G. Pon, H. Nikaido, and J. E. Hearst.** 1993. Molecular cloning and characterization of *acrA* and *acrE* genes of *Escherichia coli*. J. Bacteriol. **175:**6299–6313.
25. **Matthews, R. G., V. Massey, and C. C. Sweeley.** 1975. Identification of *p*-hydroxybenzaldehyde as the ligand in the green form of old yellow enzyme. J. Biol. Chem. **250:**9294–9298.
26. **Meng, M., W.-Q. Sun, L. A. Geelhaar, G. Kumar, A. R. Patel, G. F. Payne, M. K. Speedie, and J. R. Stacy.** 1995. Denitration of glycerol trinitrate by resting cells and cell extracts of *Bacillus thuringiensis*/*cereus* and *Enterobacter agglomerans*. Appl. Environ. Microbiol. **61:**2548–2553.
27. **Miura, K., Y. Tomioka, Y. Hoshi, H. Suzuki, M. Yonezawa, T. Hishinuma, and M. Mizugaki.** 1997. The effects of unsaturated fatty acids, oxidizing agents and Michael reaction acceptors on the induction of *N*-ethylmaleimide reductase in *Escherichia coli*: possible application for drug design of chemoprotectors. Methods Find. Exp. Clin. Pharmacol. **19:**147–151.
28. **Miura, K., Y. Tomioka, H. Suzuki, M. Yonezawa, T. Hishinuma, and M. Mizugaki.** 1997. Molecular cloning of the *nemA* gene encoding *N*-ethylmaleimide reductase from *Escherichia coli*. Biol. Pharm. Bull. **20:**110–112.
29. **Mosher, R. H., D. J. Camp, K. Yang, M. P. Brown, W. V. Shaw, and L. C. Vining.** 1995. Inactivation of chloramphenicol by *O*-phosphorylation. A novel resistance mechanism in *Streptomyces venezuelae* ISP5230, a chloramphenicol producer. J. Biol. Chem. **270:**27000–27006.

29a. **National Center for Biotechnology Information.** 16 August 1999, posting date. BLAST search engine. [Online.] http://www.ncbi.nlm.nih.gov/cgi-bin/BLAST. [27 August 1999, last date accessed.]

29b. **National Center for Biotechnology Information.** 16 August 1999, posting date. BLAST2. [Online.] http://www.ncbi.nlm.nih.gov/gorf/bl2.html. [27 August 1999, last date accessed.]

30. **Record, M. T. J., W. S. Reznikoff, M. L. Craig, K. L. McQuade, and P. J. Schlax.** 1996. *Escherichia coli* RNA polymerase ($E\sigma^{70}$), promoters, and the kinetics of the steps of transcription initiation, p. 792–821. *In* F. C. Neidhardt, R. Curtiss III, J. L. Ingraham, E. C. C. Lin, K. B. Low, B. Magasanik, W. S. Reznikoff, M. Riley, M. Schaechter, and H. E. Umbarger (ed.), *Escherichia coli* and *Salmonella*: cellular and molecular biology, 2nd ed. ASM Press, Washington, D.C.
31. **Rieger, P.-G., and H.-J. Knackmuss.** 1995. Basic knowledge and perspectives on biodegradation of 2,4,6-trinitrotoluene and related nitroaromatic compounds in contaminated soil, p. 1–18. *In* J. C. Spain (ed.), Biodegradation of nitroaromatic compounds. Plenum Press, New York, N.Y.
32. **Rohde, B. H., R. Schmid, and M. S. Ullrich.** 1999. Thermoregulated expression and characterization of an NAD(P)H-dependent 2-cyclohexen-1-one reductase in the plant pathogenic bacterium *Pseudomonas syringae* pv. glycinea. J. Bacteriol. **181:**814–822.
33. **Saito, K., D. J. Thiele, M. Davio, O. Lockridge, and V. Massey.** 1991. The cloning and expression of a gene encoding old yellow enzyme from *Saccharomyces carlsbergensis*. J. Biol. Chem. **266:**20720–20724.
34. **Sambrook, J., T. Maniatis, and E. F. Fritsch.** 1989. Molecular cloning: a laboratory manual, 2nd ed. Cold Spring Harbor Laboratory Press, Cold Spring Harbor, N.Y.
35. **Schopfer, L. M., and V. Massey.** 1991. A study of enzymes, mechanisms of enzyme action, p. 247–269. *In* S. A. Kuby (ed.), Old yellow enzyme. CRC Press, Inc., Boca Raton, Fla.
36. **Snape, J. R., N. A. Walkley, A. P. Morby, S. Nicklin, and G. F. White.** 1997. Purification, properties, and sequence of glycerol trinitrate reductase from *Agrobacterium radiobacter*. J. Bacteriol. **179:**7796–7802.
37. **Spain, J. C.** 1995. Biodegradation of nitroaromatic compounds. Annu. Rev. Microbiol. **49:**523–555.
38. **Tanner, J. J., B. Lei, S.-C. Tu, and K. L. Krause.** 1996. Flavin reductase P: structure of a dimeric enzyme that reduces flavin. Biochemistry **35:**13531–13539.
39. **Vorbeck, C., H. Lenke, P. Fischer, and H.-J. Knackmuss.** 1994. Identification of a hydride-Meisenheimer complex as a metabolite of 2,4,6-trinitrotoluene by a *Mycobacterium* strain. J. Bacteriol. **176:**932–934.
40. **Voskuil, M. I., and G. H. Chambliss.** 1998. The −16 region of *Bacillus subtilis* and other gram-positive promoters. Nucleic Acids Res. **26:**3584–3590.
41. **Voskuil, M. I., K. Voepel, and G. H. Chambliss.** 1995. The −16 region, a vital sequence for the utilization of a promoter in *Bacillus subtilis* and *Escherichia coli*. Mol. Microbiol. **17:**271–279.
42. **Warburg, O., and W. Christian.** 1933. Über das gelbe Ferment und seine Wirkungen. Biochem. Z. **266:**377–411.
43. **Wendt, T. M., J. H. Cornell, and A. M. Kaplan.** 1978. Microbial degradation of glycerol nitrates. Appl. Environ. Microbiol. **36:**693–699.
44. **White, G. F., and J. R. Snape.** 1993. Microbial cleavage of nitrate esters: defusing the environment. J. Gen. Microbiol. **139:**1947–1957.
45. **White, G. F., J. R. Snape, and S. Nicklin.** 1996. Biodegradation of glycerol trinitrate and pentaerythritol tetranitrate by *Agrobacterium radiobacter*. Appl. Environ. Microbiol. **62:**637–642.
46. **Xu, C., W. Shi, and B. P. Rosen.** 1996. The chromosomal *ars*R gene of *Escherichia coli* encodes a trans-acting metalloregulatory protein. J. Biol. Chem. **271:**2427–2432.
47. **Zenno, S., T. Kobori, M. Tanokura, and K. Saigo.** 1998. Conversion of NsfA, the major *Escherichia coli* nitroreductase, to a flavin reductase with an activity similar to that of Frp, a flavin reductase in *Vibrio harveyi*, by a single amino acid substitution. J. Bacteriol. **180:**422–425.
48. **Zenno, S., H. Koike, M. Tanokura, and K. Saigo.** 1996. Conversion of NsfB, a minor *Escherichia coli* nitroreductase, to a flavin reductase similar in biochemical properties to FRase I, the major flavin reductase in *Vibrio fischeri*, by a single amino acid substitution. J. Bacteriol. **178:**4731–4733.